IEEE Control Systems Letters paper presented at
2023 62nd IEEE Conference on Decision and Control (CDC)
December 13-15, 2023. Marina Bay Sands, Singapore

Control Framework for a UAV Slung-Payload Transportation System

Junjie Kang, Jinjun Shan, *Senior Member, IEEE*, Hassan Alkomy

***Abstract*— This paper presents a control framework for transporting a UAV slung-payload, which can asymptotically stabilize not only the UAV but also the tether swing angles. By separating the system into two subsystems, the cascade control methodology is used to design the framework, which includes two sufficient conditions and suits for a large class of existing controllers. The control framework is strictly proved with the boundness of all states such that it can guarantee the asymptotic stability of the closed-loop overall system over the entire configuration space. Then, this framework is applied to a UAV trajectory tracking control problem with stability analysis. Samples of controllers are presented in the type of saturation or dynamic feedback. Finally, numerical and experimental validations are carried out on a UAV slung-payload transportation.**

I. Introduction

In recent decades, payload transportation using tethered unmanned aerial vehicle (UAV) has attracted wide research attention due to its autonomous and flexible mobility [1]. Different from the payload grasped by UAV directly, payload transportation with the aid of tether, namely UAV slung-payload system (USPS), has several benefits such as light-weight, landing flexibility, and simple mechanism. To put USPS into practice, considerable works have been presented in [2]–[8], which can be split into maneuver/hover and trajectory/path tracking. The maneuver/hover is to transport the payload point-to-point with less tether swing motions, while the trajectory/path tracking usually follows some preplanned trajectories, even performs aerobatic flights.

Considering the principal purpose of efficient and safe aerial transportation, a large amount of research interest is focused on the former one [5]–[10]. However, it is far from simple to maneuver the USPS to target points quickly while suppressing swing angles simultaneously because of its complexly coupled dynamics. Compared to the dynamics of a single UAV, USPS becomes highly underactuated after tethering a payload to UAV [7], where the underactuated degrees increase from two to four, i.e., eight degrees of freedom with only four inputs. Thus, many promising works have been devoted to the stabilization control of the underactuated USPS [5]–[17]. For instance, in [5], a control approach for both single UAV and multiple UAVs was proposed through the linearization. In [11], the swing suppression of the USPS was studied through input shaping technique. To reject the constant disturbances, in [15], authors developed a robust IDA-PBC scheme for the USPS with a two-dimensional dynamics model. Then, to further consider the full dynamics of USPS in three-dimensional space, they proposed a model-based predictive control strategy [16], which is able to constrain the maximum swing angle. Besides, inspired by the inner-outer-loop design for UAVs [17], nonlinear controllers were designed with a hierarchical structure [7]–[9], [12], and the overall system stability was analyzed by proving the linear growth restriction of the interconnected terms between subsystems, which ensures the boundness of only actuated states rather than all states. Also, the stability of overall system can be analyzed based on the time-scale separation principle [18], which requires high control gains to ensure the fast convergence of inner-loop dynamics and to enlarge the local region of attraction. However, this might amplify measurement noises and degenerate system performance. In addition, the finite time sliding mode control for USPS based on the cascaded control design was studied in [19] with a three-loop structure. Note that most of above mentioned works linearized the system dynamics at the equilibrium or used the simplified dynamics models rather than the full dynamics of USPS [19] for stability analysis, which implies the local asymptotic stability (LAS).

Despite the satisfactory results of previous controllers with cascade system design, the boundness of the actuated states only demonstrates the stability of USPS in small operational space since the state of the outer-loop subsystem might escape to infinity because of the "peaking phenomenon" [20]. Thus, how to achieve the asymptotic stability (AS) over the entire configuration space with guaranteeing the boundness of all states still remains open. Compared to the previous studies, the main contributions of this study include the following: the full dynamics of overall USPS in three-dimensional space is considered; and the stability of closed-loop system is studied without linearization; furthermore, to ensure the AS on the entire configuration space, a simple and effective control framework is presented in the Lyapunov sense according to the cascade control design. This framework simplifies the controller design and guarantees the boundness of all state solutions of both subsystems by validating the satisfaction of two sufficient conditions. Consequently, many off-the-shelf controllers are directly applicable to the overall system with AS according to the framework. Finally, we extend the framework to the UAV trajectory tracking with the dynamic feedback controllers.

This work was supported in part by a Discovery Grant from the Natural Sciences and Engineering Research Council of Canada (NSERC), and in part by NSERC Alliance Program under Grant ALLRP 555847-20. (Corresponding author: Jinjun Shan). Authors are with the Department of Earth and Space Science and Engineering, York University, Toronto, ON M3J 1P3, Canada (e-mails: kjj@yorku.ca; jjshan@yorku.ca; h.alkomy@unb.ca).

II. Preliminary and Problem Formulation

A. Mathematical Preliminaries

Let's first consider $\sigma(s)$ a smooth and strictly increasing saturation function of class-$\mathcal{C}^2$ with bounded derivatives, and satisfying the following properties: $s\sigma(s) > 0,\ \forall s \neq 0;\ \|\sigma\| \leq d_0,\ d_0 \in \mathbb{R}^+$ and $\sigma(0) = 0$. If $s = \mathrm{col}(s_1, s_2, \cdots, s_n) \in \mathbb{R}^n$, $\sigma(s) = \mathrm{col}(\sigma(s_1), \sigma(s_2), \cdots, \sigma(s_n))$, where the notation $\mathrm{col}(\cdot)$ denotes a column vector. $\mathrm{sig}^\alpha(s) = \mathrm{sign}(s)|s|^\alpha$. If $\forall s \in \mathbb{R}^n$, then $\mathrm{sig}^\alpha(s) = \mathrm{col}(\mathrm{sig}^\alpha(s_1), \mathrm{sig}^\alpha(s_2), \cdots, \mathrm{sig}^\alpha(s_n))$.

Then, we present a lemma about cascade systems stability. Readers are referred to [21] for supplementary details.

Lemma 1: [21] Cascade system (1) is globally asymptotically stable (GAS) at the origin $(x_1, x_2) = 0$ under the conditions of: 1) Unperturbed subsystem $\Sigma_1 : \dot{x}_1 = f_1(x_1)$ is GAS at $x_1 = 0$; 2) Subsystem Σ_2 is GAS at the origin $x_2 = 0$; 3) The solution $t \mapsto (x_1, x_2)$ is bounded all the time.

$$\begin{cases} \Sigma_1 : \dot{x}_1 = f_1(x_1) + g(x_1, x_2) \\ \Sigma_2 : \dot{x}_2 = f_2(x_2) \end{cases} \tag{1}$$

where $g(x_1, x_2) = 0$ if $x_2 = 0$.

B. Dynamics Model and Problem Formulation

Considering a slung-payload connected to a UAV, the dynamic equations of USPS are given as follows [7],

$$\begin{aligned} &\dot{\xi}_1 = \xi_2 \\ &M(\xi_1)\dot{\xi}_2 + C(\xi_1, \xi_2)\xi_2 + G(\xi_1) = u \end{aligned} \tag{2}$$

$$\begin{aligned} &\dot{\Theta} = \Pi(\Theta)\omega \\ &J\dot{\omega} = -\omega \times (J\omega) + \tau \end{aligned},\ \Pi(\Theta) = \begin{bmatrix} 1 & 0 & -\mathrm{s}_\theta \\ 0 & \mathrm{c}_\phi & \mathrm{c}_\theta \mathrm{s}_\phi \\ 0 & -\mathrm{s}_\phi & \mathrm{c}_\theta \mathrm{c}_\phi \end{bmatrix} \tag{3}$$

where $\xi_1 = \mathrm{col}(q, \gamma_1, \gamma_2)$, and $q = \mathrm{col}(q_x, q_y, q_z)$ is the position vector of UAV in the inertial coordinate frame $\mathcal{F}_I$. γ_1, γ_2 are the swing angles of tether. $u = \mathrm{col}(FRe_z, 0, 0)$ is the input vector for (2), $e_z = \mathrm{col}(0, 0, 1)$ is the unit vector. $R \in \mathbb{SO}(3)$ denotes the UAV rotation matrix. $\Theta := \mathrm{col}(\phi, \theta, \psi)$ are UAV's attitude angles. F is the supplied force along the upward direction of UAV, and τ denotes the applied torque of UAV. ω is the angular velocity of UAV, and J is the inertial matrix of UAV. The variables in (2), and (3) are defined as $s_i := \sin i, c_i := \cos i, i = \{\gamma_1, \gamma_2, \phi, \theta, \psi\}$,

$M = [m_{ij}]_{n\times n}, C = [c_{ij}]_{m\times n}, m_{ij} = m_{ji},$
$m_{11} = m_{22} = m_{33} = m_q + m_p, m_{14} = m_p l c_1 c_2, m_{25} = m_p l c_2,$
$m_{12} = m_{13} = m_{23} = m_{24} = m_{45} = 0, m_{15} = -m_p l s_1 s_2,$
$m_{34} = m_p l s_1 c_2, m_{35} = m_p l c_1 s_2, m_{44} = m_p l^2 c_2^2, m_{55} = m_p l^2,$
$[c_{ij}]_{5\times 3} = 0, c_{14} = -m_p l(\dot{\gamma}_1 s_1 c_2 + \dot{\gamma}_2 c_1 s_2), c_{24} = c_{55} = 0,$
$c_{15} = -m_p l(\dot{\gamma}_1 c_1 s_2 + \dot{\gamma}_2 s_1 c_2), c_{25} = -m_p l \dot{\gamma}_2 s_2,$
$c_{34} = m_p l(\dot{\gamma}_1 c_1 c_2 - \dot{\gamma}_2 s_1 s_2), c_{35} = m_p l(\dot{\gamma}_2 c_1 c_2 - \dot{\gamma}_1 s_1 s_2),$
$c_{44} = -m_p l^2 \dot{\gamma}_2 c_2 s_2, c_{45} = -m_p l^2 \dot{\gamma}_1 c_y s_2, c_{54} = m_p l^2 \dot{\gamma}_1 c_2 s_2,$
$G = [0, 0, 0, m_p g l s_1 c_2, m_p g l c_1 s_2]^{\mathrm{T}}.$

in which m_q and m_p denote the mass of UAV and payload, respectively. l is the tether length.

Assumption 1 [7, 9]: Payload swing angles are assumed to be $(\gamma_1, \gamma_2) \in (-\pi/2, \pi/2)$, which implies the UAV will not become entangled by the tethered payload.

Problem 1: Considering the dynamics of USPS in (2) and (3) , the main goal is to design the input controller for the wrench (u, τ) to achieve USPS transporting from the start point to the target point while zeroing the swing angles, i.e.,

$$t \to \infty,\ \ \xi_1 \to \xi_{1d} = \mathrm{col}(q_d, 0, 0). \tag{4}$$

III. Control Framework For UAV Slung-Payload

A. Main Results

To achieve the control objective of the overall system of USPS, i.e., stabilization of all positions and attitudes, we view the overall system as two interconnected subsystems, as shown in Fig. 1(a). The first subsystem is the translational subsystem, which includes three positions of the UAV and two swing angles of the tethered payload. It is like an underactuated three-dimensional crane-pendulum system with five degrees of freedom but three virtual inputs, F_c. The second one is a rotational subsystem that is the attitude motion of the UAV, which is fully actuated with three torques.

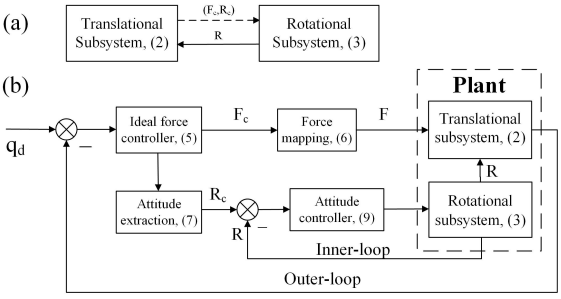

Fig. 1. Cascade Block of USPS (a) and Control Diagram (b).

As shown in Fig. 1(b), the controller is designed in two steps. First, to stabilize the translational subsystem, an ideal command force controller $F_c = \mathrm{col}(F_{cx}, F_{cy}, F_{cz})$ is designed by accommodating the force input F to the required orientation R_c. Second, the attitude of UAV is controlled through an inner-loop attitude controller τ to track the command attitudes R_c. Once the attitude errors converge to zero, the ideal command force will be generated. Consequently, a feasible attitude extraction map between F_c and F as in [22] is presented as follows,

$$F_c := FR_ce_z, \qquad R_ce_z = \begin{bmatrix} c_{\phi_c}s_{\theta_c}c_{\psi_c} + s_{\phi_c}s_{\psi_c} \\ c_{\phi_c}s_{\theta_c}s_{\psi_c} - s_{\phi_c}c_{\psi_c} \\ c_{\phi_c}c_{\theta_c} \end{bmatrix} \tag{5}$$

where $\Theta_c = \mathrm{col}(\phi_c, \theta_c, \psi_c)$ represent the desired attitude angles. Taking the fact of $\|R_ce_z\| = 1$, one can easily derive that, from (5), the magnitude of force input of UAV,

$$F = \|F_c\| \tag{6}$$

Further, by making some mathematical operations and taking the inverse of triangular functions, one can have Θ_c

as follows,

$$\begin{aligned}&\phi_c = \text{asin}[(F_{cx}s_{\psi_c} - F_{cy}c_{\psi_c})/F]\\&\theta_c = \text{atan}[(F_{cx}c_{\psi_c} + F_{cy}s_{\psi_c})/F_{cz}]\\&t \mapsto \psi_c \subset \mathcal{C}^2\end{aligned} \tag{7}$$

Here ψ_c expresses the yaw angle, namely the heading direction of UAVs. Form (7), one can solve ϕ_c, θ_c with any preassigned heading angle ψ_c. In this paper, we will consider ψ_c= 0 in the subsequent sections. It should be noted that, in general, ψ_c can be assigned freely according to a higher-level guidance demand. Then, by applying an attitude controller, one can adjust the heading angle to ψ_c.

Let's recall the translational dynamics in (2), and write the error dynamics into the cascade form as follows,

$$\dot{\xi} = f(\xi) + g(\xi, \eta) \tag{8}$$

where $\xi := \text{col}(\tilde{\xi}_1, \xi_2)$ defines the state error, and $\tilde{\xi}_1 = \xi_1 - \xi_{1d} = \text{col}(q - q_d, \gamma_1, \gamma_2)$ denotes the position error. $\xi_2 = \text{col}(\dot{q}, \dot{\gamma_1}, \dot{\gamma_2})$ is the velocity. The system's flow $f := \text{col}(f_1, f_2)$, $f_1 = \xi_2$, $f_2 = -M^{-1}(C\xi_2 + G - u_c)$. The perturbed term is $g := \text{col}(g_1, g_2)$ with $g_1 = 0$, $g_2 = M^{-1}(u - u_c)$, $u_c = \text{col}(F_c, 0, 0)$.

By introducing the following explicit input transformation

$$\tau = (\Pi^{-1}\dot{\Theta})\times(J\Pi^{-1}\dot{\Theta}) + J\dot{\Pi}^{-1}\dot{\Theta} + J\Pi^{-1}\ddot{\Theta}_c + J\Pi^{-1}\hat{\tau} \tag{9}$$

the error rotational attitude dynamics of UAV is given as

$$\dot{\eta} = \rho(\eta) = \text{col}(\dot{e}_\Theta, \hat{\tau}) \tag{10}$$

where $\eta = \text{col}(e_\Theta, \dot{e}_\Theta) = \text{col}(\Theta - \Theta_c, \dot{\Theta} - \dot{\Theta}_c)$ is the error attitude vector. $\hat{\tau}$ is the new torque in terms of η.

Then, we summarize the main theorem for stabilizing the cascade USPS (8) and (10).

Theorem 1: Cascade system (8) and (10) is GAS under the following two conditions:

P1: Design the command force F_c to make the unperturbed translational subsystem (8) GAS, and there exists a positive definite and radially unbounded function V_ξ satisfying

$$\mathcal{L}_f V_\xi \leq 0 \quad \text{and} \quad \left\| \frac{\partial V_\xi}{\partial \xi_2} \right\| \|F_c\| \leq c V_\xi, \exists c \in \mathbb{R}^+, \|\xi\| > N \in \mathbb{R}^+ \tag{11}$$

P2: Design the torque $\hat{\tau}$ to ensure the attitude subsystem (10) GAS, and there exists a positive definite function V_η for $\|\eta\| \in B(r) = \{\|\eta\| < r\} \subset \mathbb{R}, r \in \mathbb{R}^+$, that satisfying

$$\dot{V}_\eta \leq -a_\eta V_\eta^\alpha \tag{12}$$

where $a_\eta \in \mathbb{R}_+$ and $0 < \alpha \leq 1, \alpha \in \mathbb{R}^+$.

Proof: We first show the growth rate of the perturbation term $g(\xi, \eta)$ satisfying

$$\|g\| = \left\|M^{-1}(u - u_c)\right\| \leq \left\|M^{-1}\right\| \|F(R - R_c)e_z\| \leq k\|e_\Theta\| \tag{13}$$

where $k_1, k \in \mathbb{R}^+$. $\|(R - R_c)e_z\| \leq k_1\|e_\Theta\|$ has been used in (13) and the derivation is given in Appendix A.

Then, recalling (11), the Lie derivative $\mathcal{L}_g V_\xi$ is

$$\mathcal{L}_g V_\xi \leq \left\| \frac{\partial V_\xi}{\partial \xi_2} \right\| \|g(\xi, \eta)\| \leq kcV_\xi \|\eta\|, \quad \|\xi\| > N \tag{14}$$

Thus, due to GAS of (10), one has $\|\eta\| \leq \mathcal{KL}(\|\eta(0)\|, t)$, which indicates $\|\eta\|$ is bounded all the time.

Next, we continue the analysis with two situations: a) $\alpha = 1$, $\|\eta\|$ is exponential stable from (12). Then, recalling (14), we can obtain $\|\xi\|$ is bounded, see [20] for details. b) $0 < \alpha < 1$, the origin of subsystem is locally finite time stable, and there exists a finite time t_f such that $\|\eta(t)\|_{t>t_f} = 0$. Considering $V_\xi > 0$, and from (11) and (14), we have

$$\frac{d}{dt}(\ln V_\xi) \leq kc\|\eta\| \tag{15}$$

Integrating both sides of (15) , with the boundness of $\|x_2\|$ and $\|x_2(t)\|_{t>t_f} = 0$, we have

$$\ln V_\xi \leq \ln V_\xi(0) + kc\int_0^{t_f} \|\eta\| \text{dt} \leq \ln V_\xi(0) + kct_f \sup(\|\eta\|) \tag{16}$$

This indicates the boundness of V_ξ, and further implies the boundness of $\|\xi\|$. Thus, by applying Lemma 1, one can conclude that overall system is GAS under the proposed control framework.

Remark 1: Theorem 1 provides a framework to synthesize subsystem controllers, for which one can select different off-the-shelf controllers to translational and rotational subsystems. Then, by verifying conditions of P1 and P2, one can readily identify the AS of the overall system. It is very fruitful for controller design, which provides a simple and effective approach to control the underactuated USPS.

B. Sample Controllers

We first consider a homogeneous proportional-derivative (PD) controller for attitude system dynamics stabilization

$$\hat{\tau} = -k_{\tau 1}e_\Theta^\alpha - k_{\tau 2}\dot{e}_\Theta^{2\alpha/(1+\alpha)} \tag{17}$$

where $\alpha \in (0, 1]$, $\alpha \in \mathbb{R}^+$. (17) ensures the globally exponential stable for the attitude subsystem for $\alpha = 1$ and the globally finite stable while $0 < \alpha < 1$. And, it is straightforward to see the requirement of P2 in Theorem 1 is satisfied according to the Proposition 1 of [23].

Next, the translational controller, ideal force F_c, is to fulfill the requirement for the translational subsystem. We present the following sample controllers:

$$^1F_c = -k_{c1}\tilde{q} - k_{c2}\dot{q} + m_t g e_z \tag{18}$$

$$^2F_c = -k_{c1}\sigma(\tilde{q}) - k_{c2}\sigma(\dot{q}) + m_t g e_z \tag{19}$$

$$^3F_c = -k_{c1}\sigma(\tilde{q} + k_{c2}\dot{q}) + m_t g e_z \tag{20}$$

$$^4F_c = -k_{c1}\sigma\left(k_{c2}\tilde{q} + k_{c3}\sigma(\dot{q})\right) + m_t g e_z \tag{21}$$

where $k_{c1}, k_{c2}, k_{c3} \in \mathbb{R}^+$ are diagonal matrices and $m_t = m_q + m_p$. $\tilde{q} = q - q_d$ denotes the position error of UAV. (18) is a PD plus desired gravity compensation controller. (19)-(21) are (nested) saturation controllers. (19) is same as in [7] if the saturation function is specified as $\sigma(s) = \tanh(s)$. Stability analysis of the controllers is provided in Appendix B.

Remark 2: It is noteworthy that [11], [24] mainly focus on the swing suppression, where the attitude control of the quadrotor is neglected or supposed to be achieved. Thus, the

stability of overall system remains to be discussed. Similarly, in [7], [9], AS of the translational subsystem is discussed but lacks the evidence of all states boundness.

IV. Extension to UAV

In this section, we extend the proposed framework to the trajectory tracking UAV problem defined as the following.

Problem 2: For a given position trajectory $q_d(t)$ in class-$\mathcal{C}^4$ with bounded derivatives, the aim is to design a controller for the wrench (F, τ) such that

$$t \to \infty, \;\; q(t) \to q_d(t). \tag{22}$$

By zeroing the payload mass, USPS is reduced to a single UAV. Thus, the translational motion of UAV becomes

$$\ddot{q} = FRe_z/m_q - ge_z \tag{23}$$

Denoting $\chi := \mathrm{col}(\chi_1, \chi_2) = \mathrm{col}(q - q_d, \dot{q} - \dot{q}_d) \in \mathbb{R}^6$ and one can write (23) into the error dynamics as

$$\dot{\chi} = f_\chi + g_\chi \tag{24}$$

where $f_\chi = \mathrm{col}(\xi_2, F_c/m_q - ge_z - \ddot{q}_d)$, and $g_\chi = \mathrm{col}(0, F(R - R_c)e_z/m_q$. If $R = R_c$, then $g_\chi = 0$, and (24) defines the unperturbed translational subsystem.

Theorem 2: Cascaded system (24) and (10) for UAV is GAS under the prerequisites of P2 in Theorem 1 and P3.

P3: Force controller F_c ensures the unperturbed subsystem (24) GAS, and there exists a positive definite radially unbounded function V_χ and $c \in \mathbb{R}^+$ satisfying that

$$\mathcal{L}_{f_\chi} V_\chi \le 0, \left\| \frac{\partial V_\chi}{\partial \chi_2} \right\| \|F_c\| \le c V_\chi, \;\; \exists \;\; \|\chi\| > N \in \mathbb{R}^+ \tag{25}$$

Proof. Similarly, as in Theorem 1, one can have

$$\mathcal{L}_{g_\chi} V_\chi \le \left\| \frac{\partial V_\chi}{\partial \chi_2} \right\| \|g_\chi\| \le k V_\chi \|\eta\|, \;\; k \in \mathbb{R}^+ \tag{26}$$

where $\|g_\xi\| \le k_1 F \|e_\Theta\|$ has been incorporated in the second inequality. Thus, recalling P2 of Theorem 1 and its stability analysis and Lemma 1, one can conclude that GAS of the overall UAV system under P2 and P3.

Let's define a force controller F_c as,

$$F_c := \mu(\chi) + m_q g e_z + m_q \ddot{q}_d \tag{27}$$

where $\mu(\chi)$ is a feedback controller satisfying P3 that can be selected as,

$$^1\mu(\chi) = K\chi \tag{28}$$

$$^2\mu(\chi) = -k_{c1}\sigma(\chi_1) - k_{c2}\sigma(\chi_2) \tag{29}$$

$$^3\mu(\chi) = -k_{c1}\sigma(k_{c2}\chi_1 + k_{c3}\chi_2) \tag{30}$$

where $K \in \mathbb{R}^{3\times 6}$ and $k_{c1}, k_{c2}, k_{c3} \in \mathbb{R}^+$. Equation (28) is a linear PD controller given in [22]. Equations (29) and (30) are two (nested) saturation controllers meeting the P3. Stability of these controllers is straightforward from Theorem 2 and similar to the proof in Appendix B.

Furthermore, (28) is expanded into a dynamic feedback manner, such that

$$^4\mu(\bar{\chi}, \chi) = K_1\bar{\chi} + K_2\chi, \quad \dot{\bar{\chi}} = A_1\bar{\chi} + A_2\chi \tag{31}$$

where $\bar{\chi} \in \mathbb{R}^p, K_1 \in \mathbb{R}^{3\times p}, A_1 \in \mathbb{R}^{p\times p}, A_2 \in \mathbb{R}^{p\times 6}$.

Defining $z = \mathrm{col}(\bar{\chi}, \chi) \in \mathbb{R}^{p+6}$, and combing (31) with (24), we can augment the system (24) as,

$$\dot{z} = f_z + g_z = \begin{bmatrix} A_1 & A_2 \\ K_1 & K_2 \end{bmatrix} z + \begin{bmatrix} 0 \\ (FRe_z - F_c)/m_q \end{bmatrix} \tag{32}$$

The following corollary is presented for the stability of (32).

Corollary 1: Cascade system (32) and (10) for UAV is GAS under prerequisites of P2 and P4.

P4: Considering $\|F_c\| \le c_1 \|z\| + c_2, \exists \; c_1, c_2, c_3 \in \mathbb{R}^+$ ensures the unperturbed subsystem (32) GAS, and there exists a positive definite and radially unbounded function V_z satisfying that

$$\mathcal{L}_{f_z} V_z \le 0, \;\; \left\| \frac{\partial V_z}{\partial z} \right\| \|z\| \le c_3 V_z, \exists \|z\| > N \in \mathbb{R}^+ \tag{33}$$

Proof. To prove the stability, we calculate the Lie derivative,

$$\begin{aligned} \mathcal{L}_{g_z} V_z &\le \left\| \frac{\partial V_z}{\partial z} \right\| \|g_z\| \le k_1 \left\| \frac{\partial V_z}{\partial z} \right\| (c_1 \|z\| + c_2) \|e_\Theta\| \\ &\le c_4 V_z \|\eta\|, \quad \exists \|z\| > \max(N, c_2/c_1) \in \mathbb{R}^+ \end{aligned} \tag{34}$$

where $\|g_z\| \le k_1 F \|e_\Theta\|$ and $c_4 = 2kc_1c_3$. Thus, similar to the stability analysis of Theorem 1, one can conclude that GAS of the overall UAV system under P2 and P4.

V. Numerical and Experimental Results

Numerical simulation and experimental test are performed to demonstrate the effectiveness of the proposed control framework for both UAV slung-payload and UAV systems. The system parameters for simulations and experiments are chosen as: m_q=1.121 kg, m_p=0.2 kg, J=diag(0.01,0.0082, 0.0148) kg· m^2 and the tether length l=1 m.

A. Numerical Results

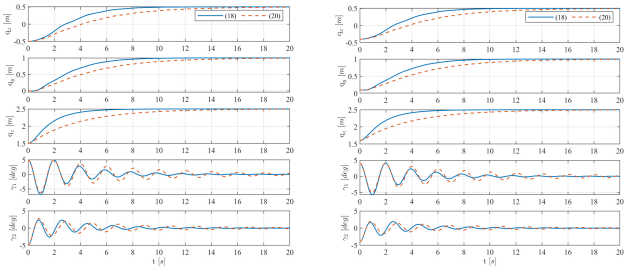

(a) (b)

Fig. 2. Responses of USPS Positions and Swing Angles: (a): $q(0)$=[-0.5, 0, 1.5], $\gamma(0)$=[5, -5]°; (b): $q(0)$=[-0.4, 0.1, 1.6], $\gamma(0)$=[3, -3]°.

We first verify the USPS with PD controller (18) and the saturation PD controller (20), in which control gains are selected as $k_{c1} = \mathrm{diag}([2, 2, 2])$ and $k_{c2} = \mathrm{diag}([4, 4, 4])$. Two cases with different initial conditions of system are simulated. In case (a), the initial position of UAV is set as $q(0) = [-0.5\,,\, 0,\, 1.5]^T$ m and target position is $q_d = [0.5\,,\, 1,\, 2.5]^T$ m. Initial angles of tether swing are $[\gamma_1(0), \gamma_2(0)] = [5, -5]^\circ$, and initial attitude angles of UAV are $\Theta_1(0) = [0, 0, 0]^\circ$. In case (b), the initial position of

UAV is set as $q(0) = [-0.4\ ,\ 0.1,\ 1.6]^T$ m. Initial angles of tether swing are $[\gamma_1(0), \gamma_2(0)] = [3, -3]^\circ$. Homogeneous attitude controller (17) is with gains $k_{\tau 1} = \text{diag}([2, 2, 2])$, $k_{\tau 2} = \text{diag}([4, 4, 4])$, and $\alpha = 0.8$. Simulation results are presented in Fig. 2, where the positions of UAV reach the desired ones successfully without overshoot and after a settling time $\approx 16s$ for both controllers under different initial conditions, while the swing angles of the payload are suppressed to zero. Note that (20) performs slightly slower transient performance than (18) due to the restriction of maximum magnitude of the input, which could be further improved by optimizing the control gains.

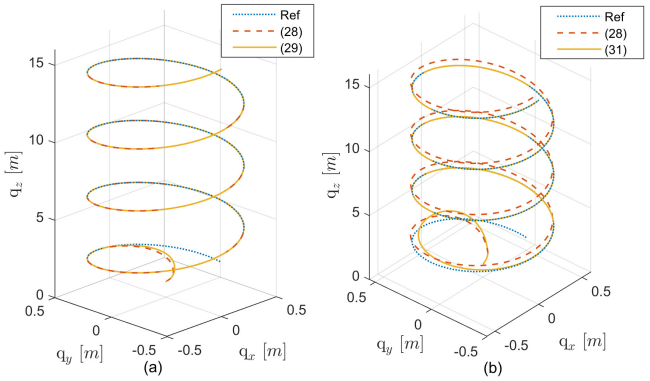

Fig. 3. UAV's Trajectories in Three-Dimensional Space: (a): Without Disturbance (d=0); (b): With Disturbance (d=0.1).

Next, two simulation cases with/without constant disturbance are carried out for UAV position tracking. A reference trajectory is given as $q_d(t) = [0.5\cos(0.05\pi t), 0.5\cos(0.05\pi t), 1 + 0.1t]^T$ m. Initial position of UAV is $q(0) = [0, 0, 1]^T$ m. In the first case, PD controller (28) with $K = -\text{diag}([2, 2, 2, 4, 4, 4])$ and saturation controller (29) are compared. Control gains of (29) and attitude controller are same as before. Initial attitudes of UAV are $\Theta(0) = [0, 10, 0]^\circ$. Trajectories of UAV are plotted in Fig. 3 in 3D space. As shown in Fig. 3(a), UAV quickly tracks the reference spiraling curve for both. Although starting with initial position biases, all position trajectories catch up the reference in a short time. Second case is a robust test, in which we consider a constant disturbance d=0.1 m/s^2 within the capacity of UAV's input acting on the position subsystem. Initial conditions are set as same as before. A dynamic feedback controller (31) (PID), $\mu = K_1\bar{\chi} + K\chi$, $\dot{\bar{\chi}} = \chi_1$, is used to compare with (28) with $K_1 = -\text{diag}([0.2, 0.2, 0.2])$. Fig. 3(b) shows that (31) presents better robust performance against the disturbance, which tracks the reference perfectly. However, for (28), there always exists a small steady error during the entire tracking process. Thus, in an external environment with disturbances, robust controllers should be considered for precise positioning.

B. Experimental Results

In the following, we setup an experimental validation on our platform of quadrotor (QDrone) referred to [4]. The dimensions of the QDrone are $40 \times 40 \times 15$ cm, and the rest of physical parameters are same as in the simulation. In this experimental test, the goal is to fly the Qdrone with a slung-payload to the target point $q_d = [1\ ,\ 0.5,\ 1.6]^T$ m. Same as in the simulation, controllers (18) and (20) are used. The experimental results are drawn in the Fig. 4, where the position errors are stabilized to zero with a settling time t_s=8.5 s and the tolerant mean average errors (MAE) of $\|q\|$ are 0.064 for (18) and 0.091 for (20) after t_s. This is consistent with the simulation that (18) performs slightly better transient performance than the saturation controller (20), and validates the effectiveness of the controller. The MAE of tether swing angels $\|\gamma\|$ are 4.34° for (18) and 4.38° for (20), and the maximum angles max$\|\gamma\|$ are 9.71° and 12.8°, respectively. Unlikely the simulation, there exist small steady errors less than 2.7° on the swing angles due to the practical turbulence and actuator vibrations. (Experimental results can be found at: https://youtu.be/8LQngOfhGb0.)

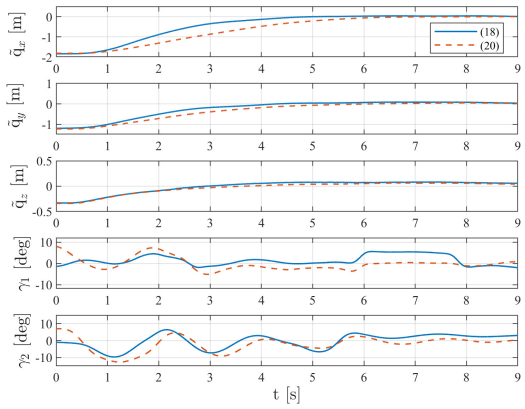

Fig. 4. Experimental Results: Position Errors and Swing Angles.

VI. Conclusions

This paper proposed a control framework to stabilize the underactuated UAV slung-payload system on the entire configuration space. By the cascade control design, the control framework was designed with two sufficient conditions that strictly guarantee the asymptotic stability of the overall closed-loop system, and simplifies the controller design and stability analysis. This control framework can be applied to many existing controllers of each subsystem for having the asymptotic stability and all state boundness. Then, the framework was extended to UAV trajectory tracking control, and dynamic feedback type of controller was presented. Simulation and experimental tests were carried out to show the effectiveness of several sample controllers. However, in the current control framework, the external time-varying disturbances, model uncertainties (payload mass and tether length), and the system time-delay have not been addressed, which could be considered in the future works to improve the system robustness and performance.

APPENDIX

A. Derivation of Inequality

$$\|(R-R_c)\,e_z\| = \left\| \begin{bmatrix} c_\phi s_\theta c_\psi + s_\phi s_\psi \\ c_\phi s_\theta s_\psi - s_\phi c_\psi \\ c_\phi c_\theta \end{bmatrix} - \begin{bmatrix} c_{\phi_c} s_{\theta_c} c_{\psi_c} + s_{\phi_c} s_{\psi_c} \\ c_{\phi_c} s_{\theta_c} s_{\psi_c} - s_{\phi_c} c_{\psi_c} \\ c_{\phi_c} c_{\theta_c} \end{bmatrix} \right\|$$

$$\leq \left\| \begin{bmatrix} |c_\psi - c_{\psi_c}| + |c_\phi - c_{\phi_c}| + |s_\theta - s_{\theta_c}| + |s_\psi - s_{\psi_c}| + |s_\phi - s_{\phi_c}| \\ |s_\psi - s_{\psi_c}| + |c_\phi - c_{\phi_c}| + |s_\theta - s_{\theta_c}| + |c_\psi - c_{\psi_c}| + |s_\phi - s_{\phi_c}| \\ |c_\theta - c_{\theta_c}| + |c_\phi - c_{\phi_c}| \end{bmatrix} \right\|$$

$$\leq \left\| \begin{bmatrix} 2\,|e_\phi| + |e_\theta| + 2\,|e_\psi| \\ 2\,|e_\phi| + |e_\theta| + 2\,|e_\psi| \\ |e_\phi| + |e_\theta| \end{bmatrix} \right\| \leq k_1 \|e_\Theta\|, \exists k_1 \in \mathbb{R}^+$$

B. Proof of Controllers

Proofs for controllers (18)-(21) are similar. For instance, we carry out the analysis for (18). Proof for (18): To analyze the stability, we take the following Lyapunov function, proposed in [7], to controller (18),

$${}^1V_\xi = \frac{1}{2}{\xi_2}^T M \xi_2 + m_p g l (1 - c_{\gamma_1} c_{\gamma_2}) + \frac{1}{2}\tilde{q}^T k_{c1} \tilde{q}$$

By taking the Lie derivative of (35), we have $\mathcal{L}_f {}^1\dot{V}_\xi = -\dot{q}^T k_{c2} \dot{q} \leq 0$. This implies ${}^1\dot{V}_\xi = 0$ as $t \to \infty$. Then, $\dot{q}$ will finally converges to the invariant set $\{\dot{q} = 0\}$. Thus, according to the detailed analysis in [7], one has the AS of unperturbed translational subsystem at the $\xi = 0$.

We further verify the second inequality in (11),

$$\left\| \frac{\partial {}^1V_\xi}{\partial \xi_2} \right\| \|F_c\| = \|M\xi_2\| \|F_c\| \leq \bar{m} \|\xi_2\| (c_1 \|\tilde{q}\| + c_2 \|\xi_2\| + m_t g)$$
$$\leq 2\bar{m} c_2 \|\xi_2\|^2 + \bar{m} c_1 (\|\xi_2\|^2 + \|\tilde{q}\|^2),\ \|\xi_2\| \geq m_t g / c_2$$
$$\leq c\, {}^1V_\xi,\ \|\xi\| > N \in \mathbb{R}^+$$

where $c = 2\max\{\bar{m}(2c_2 + c_1), \bar{m} c_1\} / \min\{\underline{m}, c_3\}$, c_1 and c_3 are the maximum and minimum eigenvalues of $\|k_{c1}\|$, respectively. c_2 are the maximum of $\|k_{c2}\|$. $\bar{m}$ and $\underline{m}$ are maximum and minimum eigenvalues of M. Thus, P1 is satisfied, and the states of the closed-loop system are bounded.

REFERENCES

[1] I. Palunko, P. Cruz, and R. Fierro, "Agile load transportation : Safe and efficient load manipulation with aerial robots," *IEEE Robotics and Automation Magazine*, vol. 19, no. 3, pp. 69–79, 2012.

[2] Z. Lv, Y. Wu, X.-M. Sun, and Q.-G. Wang, "Fixed-time control for a quadrotor with a cable-suspended load," *IEEE Transactions on Intelligent Transportation Systems*, vol. 23, no. 11, pp. 21 932–21 943, 2022.

[3] G. Yu, J. Reis, D. Cabecinhas, R. Cunha, and C. Silvestre, "Reduced-complexity active disturbance rejection controller for quadrotor-slung-load transportation," *IEEE Transactions on Systems, Man, and Cybernetics: Systems*, pp. 1–12, 2023.

[4] A. Akhtar, S. Saleem, and J. Shan, "Path following of a quadrotor with a cable-suspended payload," *IEEE Transactions on Industrial Electronics*, vol. 70, no. 2, pp. 1646–1654, 2023.

[5] M. Bernard and K. Kondak, "Generic slung load transportation system using small size helicopters," in *2009 IEEE International Conference on Robotics and Automation*, 2009, pp. 3258–3264.

[7] X. Liang, Y. Fang, N. Sun, and H. Lin, "Nonlinear hierarchical control for unmanned quadrotor transportation systems," *IEEE Transactions on Industrial Electronics*, vol. 65, no. 4, pp. 3395–3405, 2018.

[6] M. E. Guerrero-Sánchez, D. A. Mercado-Ravell, R. Lozano, and C. D. García-Beltrán, "Swing-attenuation for a quadrotor transporting a cable-suspended payload," *ISA Transactions*, vol. 68, pp. 433–449, 2017.

[8] S. Yang and B. Xian, "Exponential regulation control of a quadrotor unmanned aerial vehicle with a suspended payload," *IEEE Transactions on Control Systems Technology*, vol. 28, no. 6, pp. 2762–2769, 2020.

[9] X. Liang, Y. Fang, N. Sun, and H. Lin, "A novel energy-coupling-based hierarchical control approach for unmanned quadrotor transportation systems," *IEEE/ASME Transactions on Mechatronics*, vol. 24, no. 1, pp. 248–259, 2019.

[10] P. Pereira, J. Cortés, and D. V. Dimarogonas, "Aerial slung-load position tracking under unknown wind forces," *IEEE Transactions on Automatic Control*, vol. 66, no. 9, pp. 3952–3968, 2021.

[11] J. Potter, W. Singhose, and M. Costelloy, "Reducing swing of model helicopter sling load using input shaping," in *2011 9th IEEE International Conference on Control and Automation (ICCA)*, 2011, pp. 348–353.

[12] L. Qian and H. H. Liu, "Path-following control of a quadrotor uav with a cable-suspended payload under wind disturbances," *IEEE Transactions on Industrial Electronics*, vol. 67, no. 3, pp. 2021–2029, 2020.

[13] H. Alkomy and J. Shan, "Vibration reduction of a quadrotor with a cable-suspended payload using polynomial trajectories," *Nonlinear Dynamics*, vol. 104, no. 4, pp. 3713–3735, 2021.

[14] X. Liang, H. Lin, P. Zhang, S. Wu, N. Sun, and Y. Fang, "A nonlinear control approach for aerial transportation systems with improved antiswing and positioning performance," *IEEE Transactions on Automation Science and Engineering*, vol. 18, no. 4, pp. 2104–2114, 2021.

[15] M. Guerrero-Sánchez, O. Hernández-González, G. Valencia-Palomo, D. Mercado-Ravell, F. López-Estrada, and J. Hoyo-Montaño, "Robust ida-pbc for under-actuated systems with inertia matrix dependent of the unactuated coordinates: application to a uav carrying a load," *Nonlinear Dynamics*, vol. 105, no. 4, pp. 3225–3238, 2021.

[16] N. Urbina-Brito, M.-E. Guerrero-Sánchez, G. Valencia-Palomo, O. Hernández-González, F.-R. López-Estrada, and J. A. Hoyo-Montaño, "A predictive control strategy for aerial payload transportation with an unmanned aerial vehicle," *Mathematics*, vol. 9, no. 15, p. 1822, 2021.

[17] M.-D. Hua, T. Hamel, P. Morin, and C. Samson, "Introduction to feedback control of underactuated vtolvehicles: A review of basic control design ideas and principles," *IEEE Control Systems Magazine*, vol. 33, no. 1, pp. 61–75, 2013.

[18] Y. Xie, X. Yu, Y. Shi, and L. Guo, "Spt-based composite hierarchical antidisturbance control applied to a quadrotor uav," *IEEE Transactions on Industrial Electronics*, vol. 70, no. 1, pp. 635–645, 2023.

[19] S. Yang, B. Xian, J. Cai, and G. Wang, "Finite-time convergence control for a quadrotor unmanned aerial vehicle with a slung load," *IEEE Transactions on Industrial Informatics*, pp. 1–9, 2023.

[20] M. Jankovic, R. Sepulchre, and P. Kokotovic, "Constructive lyapunov stabilization of nonlinear cascade systems," *IEEE Transactions on Automatic Control*, vol. 41, no. 12, pp. 1723–1735, 1996.

[21] E. Sontag, "Remarks on stabilization and input-to-state stability," in *Proceedings of the 28th IEEE Conference on Decision and Control,*, 1989, pp. 1376–1378 vol.2.

[22] F. Kendoul, "Nonlinear hierarchical flight controller for unmanned rotorcraft: design, stability, and experiments," *Journal of guidance, control, and dynamics*, vol. 32, no. 6, pp. 1954–1958, 2009.

[23] S. Bhat and D. Bernstein, "Continuous finite-time stabilization of the translational and rotational double integrators," *IEEE Transactions on Automatic Control*, vol. 43, no. 5, pp. 678–682, 1998.

[24] S. Yang and B. Xian, "Energy-based nonlinear adaptive control design for the quadrotor uav system with a suspended payload," *IEEE Transactions on Industrial Electronics*, vol. 67, no. 3, pp. 2054–2064, 2020.